7012–7027 Nucleic Acids Research, 2014, Vol. 42, No. 11 Published online 14 May 2014
doi: 10.1093/nar/gku413

Ligand-dependent corepressor contributes to transcriptional repression by C_2H_2 zinc-finger transcription factor ZBRK1 through association with KRAB-associated protein-1

Mario R. Calderon[1], Mark Verway[1], Radia Ouelaa Benslama[2,3], Mirela Birlea[3], Manuella Bouttier[1], Vassil Dimitrov[1], Sylvie Mader[2,3] and John H. White[1,4,*]

[1]Department of Physiology, McGill University, Montreal, QC, Canada, [2]Department of Biochemistry, Université de Montréal, Montreal, QC, Canada, [3]Institut de Recherche en Immunologie et Cancérologie (IRIC), Université de Montréal, Montreal, QC, Canada and [4]Department of Medicine, McGill University, Montreal, QC, Canada

Received August 21, 2013; Accepted April 24, 2014

ABSTRACT

We identified a novel interaction between ligand-dependent corepressor (LCoR) and the corepressor KRAB-associated protein-1 (KAP-1). The two form a complex with C_2H_2 zinc-finger transcription factor ZBRK1 on an intronic binding site in the growth arrest and DNA-damage-inducible α (*GADD45A*) gene and a novel site in the fibroblast growth factor 2 (*FGF2*) gene. Chromatin at both sites is enriched for histone methyltransferase SETDB1 and histone 3 lysine 9 trimethylation, a repressive epigenetic mark. Depletion of ZBRK1, KAP-1 or LCoR led to elevated *GADD45A* and *FGF2* expression in malignant and non-malignant breast epithelial cells, and caused apoptotic death. Loss of viability could be rescued by simultaneous knockdowns of *FGF2* and transcriptional coregulators or by blocking FGF2 function. FGF2 was not concurrently expressed with any of the transcriptional coregulators in breast malignancies, suggesting an inverse correlation between their expression patterns. We propose that ZBRK1, KAP-1 and LCoR form a transcriptional complex that silences gene expression, in particular *FGF2*, which maintains breast cell viability. Given the broad expression patterns of both LCoR and KAP-1 during development and in the adult, this complex may have several regulatory functions that extend beyond cell survival, mediated by interactions with ZBRK1 or other C_2H_2 zinc-finger proteins.

INTRODUCTION

Eukaryotic gene transcription is controlled by epigenetic changes and chromatin reorganization, which are mediated by sequence-specific transcription factor (TF) binding to proximal or distal regulatory elements (1,2). While TFs bind deoxyribonucleic acid (DNA) directly, they do not possess the catalytic activities required to modify the amino acid residues of N-terminal histone tails, and hence cannot affect the structure of chromatin. However, they provide a platform on to which coactivators or corepressors bind, and either directly modify histone tails or recruit additional proteins that do so (3). The result of these interactions is the formation of transcriptional complexes on DNA that can number up to 50 proteins (4), which dictate a specific transcriptional outcome, ultimately altering cell function (2).

The coregulator ligand-dependent corepressor (LCoR) binds directly to ligand-bound nuclear receptors through an N-terminal NR-box (LxxLL motif) and represses hormone-stimulated transactivation via recruitment of histone deacetylases (HDACs), C-terminal binding proteins (CtBPs) (5–7) and indirect association with CtBP-interacting protein (7). It also binds to Krüppel-like factor 6 (KLF6) to repress KLF6 target genes (8), indicating that it can associate with multiple classes of TFs. LCoR is expressed very early in embryonic development and widely in the adult (5). Another broadly expressed corepressor is Krüppel-associated box (KRAB)-associated protein 1 (KAP-1; also known as TRIM28). KAP-1 is predominantly associated with intronic regions of specific genes where it mediates transcriptional repression by recruitment of the histone methyltransferase SET domain, bifurcated 1 (SETDB1), which catalyzes histone 3 lysine 9 tri-methylation (H3K9me3) (9–12). The N-terminal region of KAP-1 contains an RBCC (Really Interesting New Gene finger, two B-box zinc fingers and a coiled-coil) do-

*To whom correspondence should be addressed: Tel: +1 514 398 8498; Fax: +1 514 398 7452; Email: john.white@mcgill.ca

main which mediates its recruitment to chromatin through associations with the KRAB domain of a variety of C_2H_2 zinc-finger TFs (13).

Here, we report the results of a yeast two-hybrid screen using LCoR as bait, which identified KAP-1 (also known as tripartite motif 28; TRIM28) as an LCoR-binding partner, potentially linking LCoR to transcriptional repression by an array of C_2H_2 TFs. We investigated the putative roles of LCoR in repression of transcription by C_2H_2 TFs using zinc finger and BRCA1-interacting protein with a KRAB domain [ZBRK1; also known as zinc-finger protein (ZNF) 350], as a model, as ZBRK1 binds KAP-1 (14–16) and has a variety of defined targets including growth arrest and DNA-damage-inducible α (*GADD45A*) (17), high motility group A-T hook 2 (*HMGA2*) (18), matrix metalloproteinase 9 (*MMP9*) (19) and angiopoietin 1 (*ANG1*) (20). ZBRK1 binds to both promoter and intragenic regions. Moreover, depending on the context, ZBRK1 may promote or hinder the development of certain types of cancer (17–20). We find that a complex composed of LCoR, KAP-1 and ZBRK1 binds to an intronic motif and represses expression of *GADD45A* across all cell lines investigated. In addition, we found a novel ZBRK1 target gene, *FGF2* (fibroblast growth factor-2), repressed by the transcriptional complex in MCF-7 breast adenocarcinoma and MCF10A breast epithelial cells through binding to a nearly identical 3′ intronic motif and establishing the H3K9me3 repressive mark with which the histone methyltransferase SETDB1 is associated. FGF2 has been shown to inhibit MCF-7 cell growth (21,22) and downregulate levels of Bcl-2, promoting apoptosis (23). Similarly, in T47D ductal carcinoma cells (24), forced FGF2 expression conferred a less malignant phenotype. Remarkably, ablation of ZBRK1, KAP-1 or LCoR markedly increased MCF-7 and MCF10A cell apoptosis, an effect inhibited by blocking FGF2 expression or function. Expression patterns of FGF2 and the three transcriptional regulators were mutually exclusive in a variety of malignant breast tissues, offering a potential molecular mechanism for low FGF2 expression in certain types of breast cancer (25–28). In conclusion, we propose that a complex composed of LCoR, KAP-1 and C_2H_2 zinc-finger TF ZBRK1 promotes a transcriptional program that silences gene expression which, among other potential outcomes, suppresses FGF2-induced apoptosis.

MATERIALS AND METHODS

Note that at least three independent biological replicates of all experiments were performed and one representative set of experiments was chosen for presentation in figures unless otherwise indicated below. Values reported are mean + SD.

Isolation of KAP-1 cDNA sequence

A yeast two-hybrid screen (1.4×10^6 transformants; BD Biosciences human fetal brain MATCHMAKER cDNA library HL4028AH; Mountain View, CA, USA) with an open reading frame (ORF) of LCoR yielded 32 $His^+/LacZ^+$ colonies. Two colonies contained ∼650–850-bp inserts corresponding to KAP-1. Homologies to human genomic sequences were found as previously described (8).

Recombinant plasmids

pcDNA3.1-FLAG-LCoR-433 has been previously described (8), pcDNA3-HA-KAP-1 and pCMV-Tag3B-ZBRK1 were kind gifts from Dr Muriel Aubry (Université de Montréal) and Dr David K. Ann (City of Hope Medical Center, Duarte), respectively. The reporter gene constructs were generated by cloning a polymerase chain reaction (PCR)-amplified fragment of the intronic regions of *FGF2* and *GADD45A* with EcoRI and BamHI restriction digestion sites into the pCLuc Mini-TK2 vector (New England Biolabs).

Antibodies and reagents

A custom antibody against LCoR has previously been described (8). Antibodies for LCoR (sc-134674) and β-actin (sc-47778) and suramin sodium (sc-200833) were purchased from Santa Cruz Biotechnology (Santa Cruz, CA, USA). Antibodies for HA (ab1424), ZBRK1 (ab77085), KAP-1 (ab10483) and SETDB1 (ab12317) were purchased from Abcam (Cambridge, MA, USA). Antibodies for FLAG (F1804) and FGF2 (F5180) were purchased from Sigma (St-Louis, MO, USA). The antibody for H3K9me3 (05-1242) was purchased from Millipore (Billerica, MA, USA). The mouse antibody for KAP-1 was a kind gift from Dr Muriel Aubry (Université de Montréal) (29).

Cell culture

MCF-7, T47D and MCF10A cells were obtained from the American Type Culture Collection (ATCC). MCF-7 cells were cultured in Dulbecco's modified Eagle's medium (319-005-CL, Multicell) supplemented with 10% Fetal Bovine Serum (FBS). T47D cells were cultured in RPMI-1640 (350-005-CL, Multicell) supplemented with 10% FBS. MCF10A cells were cultured according to ATCC guidelines with a kit (Lonza, CC-3150) supplemented with cholera toxin (C8052, Sigma) at a concentration of 10 ng/ml. All experiments were carried out between passage numbers 5 and 25.

GST pull-down assays and immunoprecipitation

Glutathione S-transferase (GST) pull-downs were performed using the MagneGST™ Pull-Down System (Promega, WI, USA). Immunoprecipitations were performed as previously described (8). Samples were immunoprecipitated with α-IgG, α-HA (ab1424 or custom) or α-FLAG (F1804).

Chromatin immunoprecipitation and reChIP assays

Chromatin immunoprecipitation (ChIP) and reChIP assays were performed essentially as previously described (8). Immunoprecipitations were performed with corresponding antibodies (ab77085, ab10483, sc-134674) and two sets of specific and one set of non-specific (NS) primer sequences as well as an additional set for H3K9me3, which is detailed in Supplementary Table S1, were used to validate protein binding.

Luciferase reporter gene assays

Luciferase reporter gene assays were performed as previously described (8) with the exception that the BioLux Cypridina Luciferase Assay Kit (E3309L, New England Biolabs) was used. All assays were normalized to β-gal activity.

siRNA knockdowns

siRNAs for LCoR (HSC.RNAI.N001170765.12.1/3), ZBRK1 (HSC.RNAI.N021632.12.1/2), KAP-1 (HSC.RNAI.N005762.12.1/2), FGF2 (HSC.RNAI.N002006.12.3) and MMP9 (HSC.RNAI.N04994.12.2) were purchased from Integrated DNA Technologies (Coralville, IA, USA). Knockdowns were performed essentially as previously described (8). Briefly, MCF-7/MCF10A/T47D cells were plated in 6-wells plates. Cells were transfected in OPTIMEM (GIBCO) with corresponding siRNA for 5 h (MCF-7/MCF10A/T47D) and 8 μl of Lipofectamine RNAI Max (Invitrogen). After this incubation, media was added, and cells were allowed to recover for 72 h after which they were collected following standard protocols. Messenger ribonucleic acid (mRNA) expression analysis was carried out by quantitative real time PCR (RT-qPCR).

Enzyme-linked immunosorbent assay

FGF2 secretion in MCF-7 cell media supernatant was measured with an FGF2 enzyme-linked immunosorbent assay (ELISA) kit (KHG0021, Invitrogen). Briefly, siRNA-mediated knockdowns were performed as previously described. The media was supplemented with a protease inhibitor cocktail (P1860, Sigma) at a 1:600 concentration. After a 48/72-h recovery from the end of transfection, media supernatant was collected and centrifuged for 10 min at 1000 rpm. The ELISA was then performed according to the manufacturer's instructions. Results were then normalized to the corresponding cell numbers.

Cytotoxicity detection

Cytotoxicity of cells after siRNA-mediated knockdowns was measured using a Cytotoxicity Detection Kit Lactate dehydrogenase (LDH) assay, (Cat. No.11 644 793 001, Roche). Briefly, siRNA-mediated knockdowns were performed as previously described in 12-well plates. After a 65-h recovery period, media supernatant was collected and centrifuged for 5 min at 2600 rpm at room temperature. Samples were diluted 2:3 in water and the assay was then performed according to the manufacturer's instructions. The low control used was mock transfected cells, while the high control was mock transfected cells lysed with 1% Triton-X. Three independent biological experiments were performed in triplicate, and data were pooled for figure production.

Cell death ELISA

Apoptosis or necrosis was detected after siRNA-mediated knockdowns with the Cell Death Detection ELISA^{PLUS} (11 774 425 001, Roche). Briefly, siRNA-mediated knockdowns were performed in 96-well plates in sextuplets. After a 26 or 65-h recovery period, the assay was performed according to the manufacturer's instructions. The kit detects enrichment of mono- and oligonucleosomes caused by DNA fragmentation and is supplied with a positive control, which was also reported in the figure, while the negative control was mock transfected cells.

Caspase 3/7 activity

Caspase 3/7 activity after siRNA-mediated knockdowns was measured with the Caspase-Glo® 3/7 assay (G8091, Promega). Briefly, siRNA-mediated knockdowns were performed in white-walled 96-well luminometer plates. After a 24/65-h recovery period, the assay was performed according to the manufacturer's instructions. Luminescence results were normalized to the luminescence from mock transfected cells and then calculated as a fold change from the scrambled control activity.

FGF2 inhibitor

siRNA-mediated knockdowns were performed as previously described in 12-well plates. After a 65-h recovery period in media containing suramin sodium at 100 μM or control, an LDH assay was performed.

Imaging

Cells were grown in 6-well plates and siRNA-mediated knockdowns were performed as previously described. After a 48-h recovery period, cells were washed with phosphate buffered saline and then fresh media was added. Two hundred microliters of Trypan Blue was added to each well and images were taken using an AMG Evos Core XL microscope. Cell counts were calculated according to three independent images taken of each condition.

RNA isolation, cDNA synthesis and RT-qPCR

RNA isolation, cDNA synthesis and RT-qPCR were performed as previously described (8). The primers that were used are detailed in Supplementary Table S1.

Tissue microarrays

Immunostaining with antibodies was performed using a Discovery XT automated immunostainer (Ventana Medical Systems Roche Group, Tucson, AZ, USA). Antigen retrieval was conducted with citrate buffer pH 6.0 for 40 min at room temperature. Antibody (1/50) was incubated for 60 min on every section (BR1006, US Biomax) at room temperature. Sections were then incubated with a biotinylated antibody against specific IgG for 30 min at room temperature. Streptavidin coupled to horseradish peroxidase and 3,3′-diaminobenzidine were used according to the manufacturer's instructions (DABmap kit, Ventana Medical Systems Roche Group, Tucson, AZ, USA). Tissue sections were counterstained with hematoxylin. Digital brightfield slides were acquired with NanoZoomer® 2.0-HT scanner

(Hamamatsu Photonics K.K., Japan) at ×40 magnification. Images were captured with NDP.view 1.2.25 free Hamamatsu viewer software and used to score the Tissue Microarrays (TMAs) with a previously described method (30).

Statistical analysis

Statistical analysis was carried out with the software SYSTAT10.1 by performing the indicated tests, and figures were produced with the software Photoshop. Probability values are as follows: * ≤0.05, ** ≤0.01 and *** ≤0.001.

Access and analysis of TCGA data set

A publicly available The Cancer Genome Atlas (TCGA) data set [breast invasive carcinoma (BRCA)-UNC-IlluminaHiSeq_RNAseq, $N = 1106$] was downloaded via the Cancer Genome Atlas data portal (https://tcga-data.nci.nih.gov/tcga/). We analyzed the TGCA data using the UCSC Cancer Browser. Normalizing the expression of genes in the data set to normal tissue, we saw that FGF2 expression is reduced in breast invasive carcinoma, while TRIM28 is up, and ZNF350 and LCoR show no difference (not shown). Gating on breast cancer cells that have a low or high expression of FGF2, we can see that the distribution of KAP-1 and ZBRK-1 expression, but not LCoR, is inversely correlated with the expression of FGF2 in the samples of breast invasive carcinoma (Figure 8). In cases where FGF2 was elevated, the mean expression of KAP-1 and TRIM28 was negative, and the statistical significance of this inverse correlation was significant to –log(−3) or $P = 0.001$ as determined by student's *t*-test.

RESULTS

LCoR interacts with corepressor KAP-1

The early and widespread expression of LCoR (5) and its presence in and regulation of various types of multiprotein transcriptional complexes (4,5,8,31) suggest that it is a multi-functional coregulator. Given its high expression in human fetal brain (5), we screened a human fetal brain yeast 2-hybrid cDNA library with a construct containing the Gal4 DNA binding domain (147 amino acids) and full-length LCoR (Supplementary Figure S1A), and identified two independent ∼650–850-bp-long clones encoding the C-terminal region of KAP-1, a widely expressed transcriptional coregulator (13). These clones encompass amino acids 453-670 and 453-737, respectively (Figure 1A, top). To confirm the association of LCoR with KAP-1 we analyzed their interactions in MCF-7 cells, which express both proteins (Supplementary Figure S1B). MCF-7 cells were transfected with either HA-tagged KAP-1 or FLAG-tagged LCoR, checked for expression of the tagged proteins (Figure 1B, upper panels), immunoprecipitated with either anti-HA or anti-FLAG antibody and then probed for LCoR or KAP-1 (Figure 1B, middle panels). An interaction between endogenous proteins was also detected by immunoprecipitating KAP-1 and then probing for LCoR in MCF-7 cells (Figure 1B, lower panel). The association was further validated by pull-downs using GST fusions of KAP-1 or the estrogen receptor α (ERα) ligand binding domain as a positive control (Figure 1C). Additional pull-downs with GST fusions of full-length or truncated LCoR revealed that KAP-1-bound to the C-terminal domain (a.a. 302 to 433) of LCoR (Figure 1C; note that the GST fusions of truncated LCoR mutants were produced in bacteria at far higher levels than GST fused to full-length LCoR). The 302-433 region of LCoR identified is distinct from the central domain required for interaction with HDACs (6) and the tandem N-terminal P*X*DLS consensus motifs required for binding of CtBP corepressors (5). Finally, as KAP-1 interacts with C_2H_2 zinc-finger TF ZBRK1, which functions as a transcriptional repressor in MCF-7 cells (15), we were interested in determining whether LCoR was a component of a KAP-1/ZBRK1 complex. HA-tagged KAP-1 co-immunoprecipitated with endogenous ZBRK1 in MCF-7 cells (Figure 1D, left panel), as previously reported (14–16). Similarly, immunoprecipitation of transiently expressed FLAG-LCoR (Figure 1D, right panel) revealed that LCoR and ZBRK1 also co-immunoprecipitate.

ZBRK1, KAP-1 and LCoR repress *FGF2* and *GADD45A* gene expression in breast cancer cells

Previous microarray analysis in non-tumorigenic MCF10A cells provided evidence that ZBRK1 targets *ANG1* and potentially *FGF2* (20), while other experimental work established targets *GADD45A* (17), *HMGA2* (18) and *MMP9* (19). To determine if these genes are regulated by a transcriptional complex containing ZBRK1-KAP1-LCoR, we performed knockdowns of each protein in MCF10A and MCF-7 cells, which express all three proteins (Figure 2A, Supplementary Figures S1B and 2A, top). RT-qPCR analysis revealed that ablation of any of the components enhanced expression of *GADD45A, HMGA2, MMP9 and FGF2* in MCF10A cells, but did not affect *ANG1* expression (Figure 2B). In MCF-7 cells, none of the knockdowns affected expression of *ANG1* or *HMGA2*, whereas expression of *GADD45A* and *MMP9* was enhanced, although the effect of LCoR depletion on *MMP9* expression was not significant (Figure 2C). Note that *HMGA2* expression in MCF-7 cells was at the limit of detection. Notably, knockdowns also led to strongly enhanced *FGF2* expression in MCF-7 cells (Figure 2C). We confirmed the effects of knockdowns on *FGF2* and *GADD45A* expression in MCF-7 cells with a second independent set of siRNAs (Supplementary Figure S2B). As a control, we also knocked down the expression of another TF, Forkhead box O3A (FoxO3A), chosen because FoxO3A enhances *GADD45A* expression (32). Ablation of FoxO3A led to a nearly 60% decrease in *GADD45A* mRNA but no change in *FGF2* expression (Supplementary Figure S2C). To further explore the role of LCoR, KAP-1 and ZBRK1, we performed knockdowns in T47D breast ductal carcinoma cells, which express all three proteins (Supplementary Figures S1B and S2A). *GADD45A* was expressed in T47D cells, and ablation of any of the transcriptional regulators enhanced its expression (Figure 2D). In contrast, *FGF2* transcripts were not detected, consistent with other findings (23), and none of the siRNA knockdowns lead to detectable expression (data not shown). Similarly, no induction of *MMP9* expression

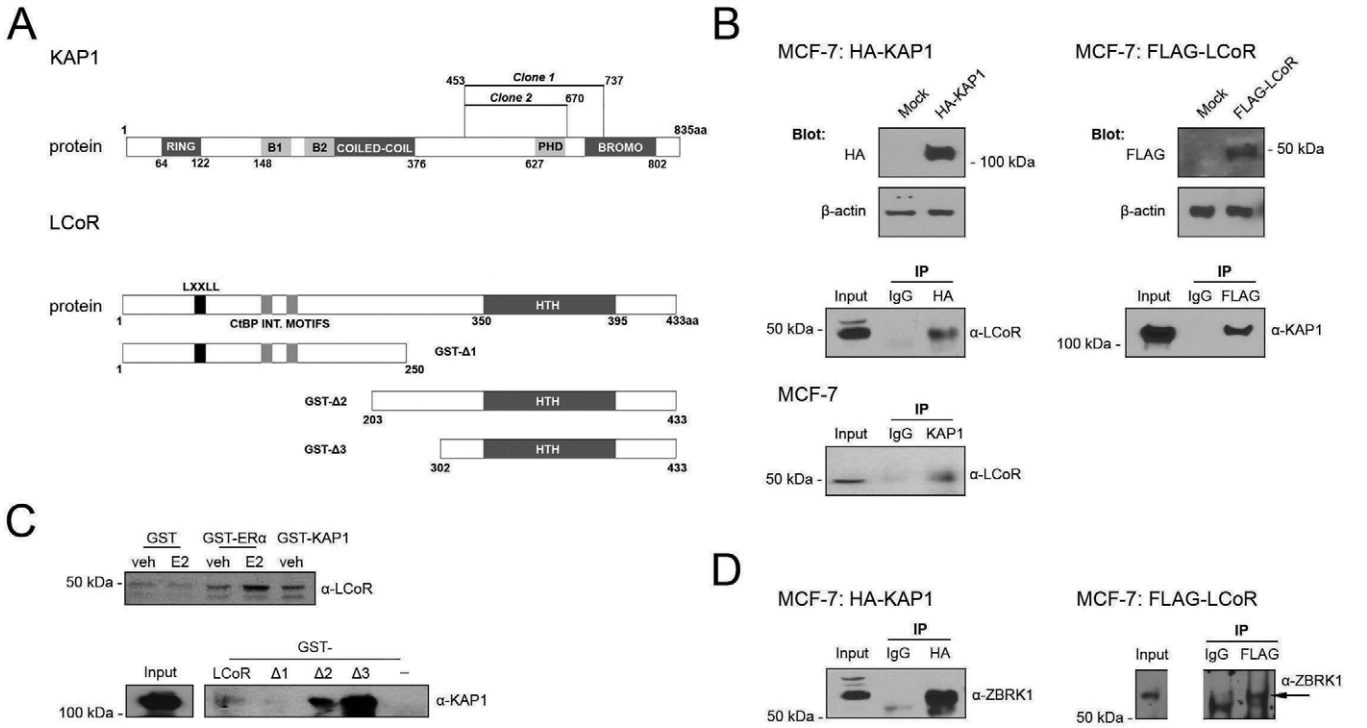

Figure 1. Identification and confirmation of interaction between transcriptional complex components. (**A**) Top: schematic representation of the two KAP-1 cDNA clones identified with the yeast two hybrid. Bottom: LCoR truncation mutants used in this study. (**B**) Upper panels: MCF-7 cells were transfected with pcDNA3.1FLAG-LCoR or pCDNA3-HA-KAP-1 and western blots (WB) were performed to confirm expression of transiently transfected HA-KAP1/FLAG-LCoR. Middle left panel: HA was immunoprecipitated from MCF-7 cells and immunoprecipitates were probed for LCoR. Middle right panel: FLAG was immunoprecipitated followed by a western blot for KAP-1. Lower right panel: co-immunoprecipitation of endogenous LCoR and KAP-1 in MCF-7 cells. KAP-1 was immunoprecipitated with specific antibody followed by a western blot for LCoR. (**C**) Results of LCoR/KAP-1 WB of pull-downs with GST control or fusions with full-length LCoR/KAP-1 or truncated LCoR mutants described in (A) and *in vitro* translated LCoR or KAP-1. Note that the input for the KAP-1 western blot is from a shorter exposure of the same gel. The known interaction of LCoR and the estrogen receptor α (ERα) was used as a positive control. (**D**) MCF-7 cells were transfected as previously described and immunoprecipitations were carried out with HA/FLAG and probed for ZBRK1. Due to the intensity of the signal from the IP, different exposures were performed for the input (high) and IP (low) for the same result.

was observed under any conditions (Figure 2D). However, its expression was at the limit of detection by RT-qPCR.

ZBRK1, KAP1 and LCoR colocalize on intronic binding sites in *FGF2* and *GADD45A* genes

ZBRK1 recognizes a consensus motif GGGxxxCAGxxxTTT, which is present between exons 3 and 4 of the *GADD45A* gene (Figure 3A, top) (17). ChIP assays on the intronic *GADD45A* sequence in MCF-7 cells revealed that ZBRK1, KAP-1 and LCoR bind to this region (Figure 3A, left panel). Moreover, re-ChIPs, consisting of an immunoprecipitation (IP) for ZBRK1 followed by a second IP for either KAP-1 or LCoR, revealed that LCoR and KAP-1 co-associate with ZBRK1 at this location (Figure 3A, right panel). Scanning the promoter (∼10 kb upstream) and intragenic region of the *FGF2* gene (∼70 kb) with the 'DNA pattern' tool (http://www.rsat.eu/) revealed essentially identical putative ZBRK1 sequence motifs between exons 1 and 2 (Figure 3B, top) and between exons 2 and 3 (Figure 3C, top). Similar ChIP and re-ChIP experiments confirmed that ZBRK1, KAP-1 and LCoR bound together to the first region (exons 1 and 2; Figure 3B), but not the second (exons 2 and 3; Figure 3C). To establish specificity of enrichment observed in ChIP and re-ChIP experiments, we performed qPCR analyses with primers encompassing an NS sequence (NS; Figure 3A and B), which failed to detect binding (Supplementary Figure S3A and B).

To further analyze the function of these repressor complexes, we tested for the presence of histone methyltransferase SETDB1, which catalyzes the establishment of the epigenetic silencing mark H3K9me3 and is associated with KAP-1 function (12,13). ChIP assays revealed that SETDB1 was associated with both intronic regions bound by ZBRK1/KAP-1/LCoR in MCF-7 cells (Figure 4A). Moreover, the H3K9me3 mark was modestly enriched in *GADD45A* and *FGF2* intronic regions bound by ZBRK1/KAP-1/LCoR in MCF-7 cells (Figure 4B). Notably, strong enrichment of H3K9me3 was observed at the ZBRK1 motif in the *GADD45A* gene in T47D cells (Figure 4B), but not at the motif in the *FGF2* gene, whose expression was not detected and not induced upon ablation of ZBRK1, KAP-1 or LCoR in T47D cells (Figure 2). In control experiments, qPCR analyses targeting a genomic region with no evidence of H3K9me3 failed to detect enrichment (Figure 4C). As their ablation compromises MCF-7 cell viability (Figure 5), ZBRK1, KAP-1 or LCoR expression was knocked down in T47D cells. This depleted H3K9

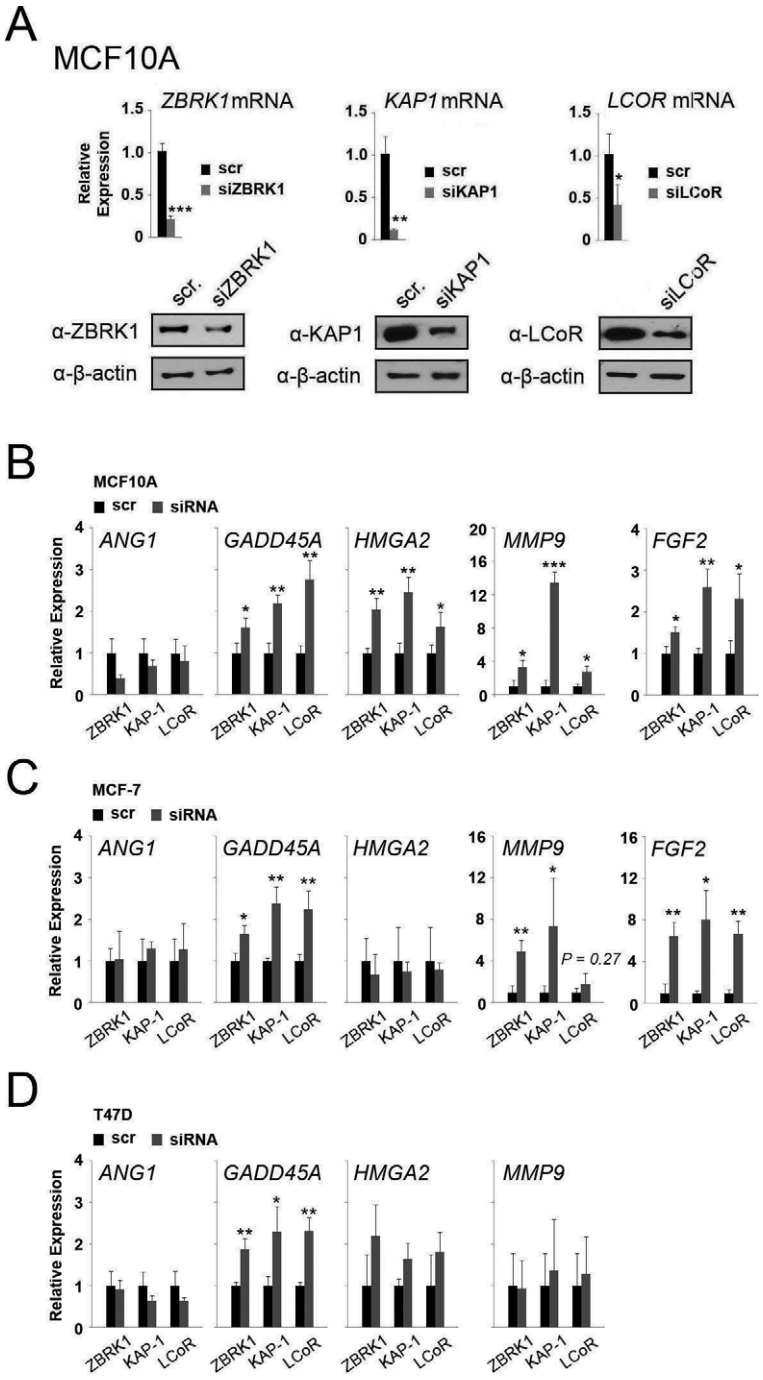

Figure 2. LCoR, KAP-1 and ZBRK1 regulate *FGF2* and *GADD45A* expression. (**A**) siRNA-mediated knockdowns in MCF10A cells were performed for ZBRK1, KAP-1 and LCoR. mRNA was measured by RT-qPCR and WB was performed following standard protocols. Gene expression analysis of *ANG1*, *HMGA2*, *MMP9*, *GADD45A* and *FGF2* by RT-qPCR following gene knockdowns in MCF10A (**B**), MCF-7 (**C**) and T47D cells (**D**). Two-sample *t*-tests were performed to determine statistical significance in all cases.

tri-methylation on *GADD45A* (Figure 4D), consistent with the role of KAP-1-containing complexes recruiting histone methyltransferase activity. Taken together, these data show that binding of the ZBRK1/KAP-1/LCoR complex to cognate motifs is associated with H3K9 tri-methylation and the presence of methyltransferase SETDB1.

To further substantiate the regulatory role of the novel ZBRK1 motif identified between exons 1 and 2 in the *FGF2* gene, we analyzed the *FGF2* genomic region in the H3K9me3 ChIPseq MCF-7 data set from the Encyclopedia of DNA elements (ENCODE) (33). This revealed a series of H3K9me3 peaks in the exon 1–2 region, one of which encompasses the element that binds ZBRK1, KAP-1 and LCoR (Figure 4E, Region 1 box). Notably, no peaks were found in the exon 2–3 region containing the putative but non-functional ZBRK1 element examined above (Fig-

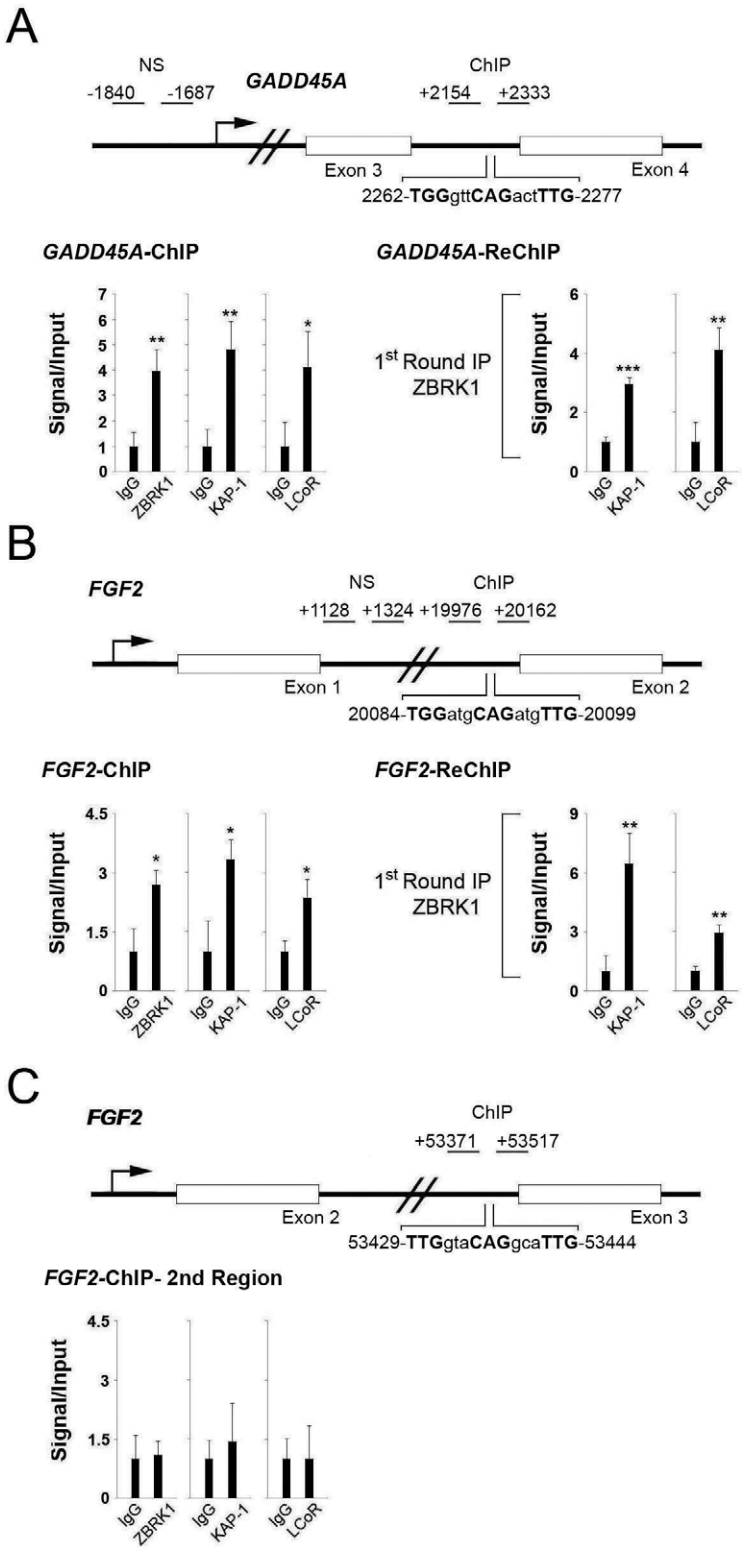

Figure 3. Analysis of ZBRK1, KAP-1 and LCoR binding to intronic ZBRK1 motifs in the *GADD45A* and *FGF2* genes by ChIP assay. Top: schematic representations of the *GADD45A* (**A**) or *FGF2* (**B**) and (**C**) gene sections analyzed by ChIP. Regions amplified encompassing the ZBRK1 recognition sequence and non-specific (NS) control sequences are indicated. Left: ChIP assays were performed in MCF-7 cells with ZBRK1, KAP-1 and LCoR antibodies followed by qPCR with specific primers for the *GADD45A* (A) or *FGF2* (B) and (C) intronic regions. Right: results of re-ChIP assays in MCF-7 cells are shown, in which a first round of ChIP for ZBRK1 followed by a second round of immunoprecipitation for KAP-1 or LCoR was performed, followed by qPCR with specific primers for the *GADD45A* (A) or *FGF2* (B) intronic regions. Student's *t*-tests were performed to ascertain statistical significance.

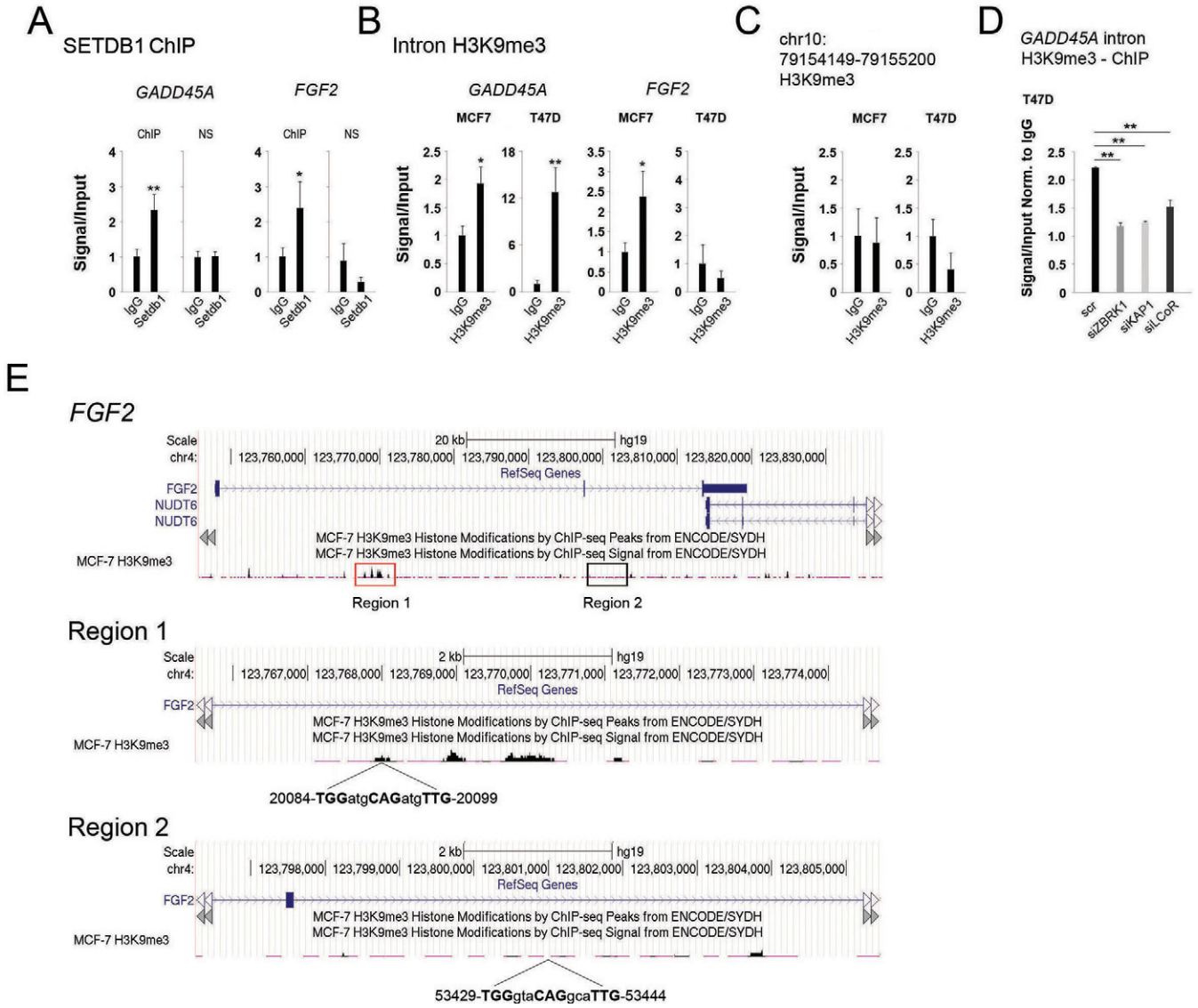

Figure 4. The histone methyltransferase SETDB1 binds intragenic regions in *GADD45A* and *FGF2* that are enriched for H3K9me3. (**A**) Results of a ChIP assay in MCF-7 cells with a SETDB1 antibody followed by qPCR with specific and NS primers for the *GADD45A* (left) or *FGF2* (right) intronic regions. (**B**) Results of ChIP assays in MCF-7 or T47D cells with an H3K9me3 antibody followed by qPCR with specific primers for the *GADD45A* (left) or *FGF2* (right) intronic regions. (**C**) Negative control for H3K9me3 enrichment. ChIP assay with anti-H3K9me3 antibody followed by qPCR analysis with primers (H3K9-Nme in Supplementary Table S1) directed toward genomic region chr10:79154149-79155200 with no evidence of H3K9me3 in MCF-7 cells as found with the ENCODE USC Genome browser GRCh37/hg19 Assembly. Two-sample *t*-tests were performed to ascertain statistical significance on all assays. (**D**) Knockdown of ZBRK1, KAP-1 or LCoR in T47D cells followed by ChIP assay for the H3K9me3 mark and qPCR with specific primers. An analysis of variance (ANOVA) followed by the Tukey test was performed to ascertain statistical significance. (**E**) ENCODE data showing the H3K9me3 methylation patterns of the *FGF2* regions studied in Figures 3 and 4. Region 1 contains the *FGF2* ZBRK1 motif that binds components of the ZBRK1/KAP-1/LCoR complex, whereas Region 2 encompasses the motif that failed to bind the complex (see Figure 3).

ure 4E, Region 2 box). This provides independent verification that the exon 1–2 motif is associated with elevated H3K9 methylation.

We also generated luciferase reporter gene constructs containing ~500-bp intronic fragments of *FGF2* or *GADD45A* encompassing the ZBRK1 binding motifs, inserted upstream of a minimal herpes simplex virus type 1 thymidine kinase (TK) promoter that was not repressed by the three proteins (Supplementary Figure S4A and B). Transient transfection of ZBRK1, KAP-1 or LCoR expression vectors revealed a dose-dependent reduction in expression of reporter constructs containing either the *FGF2* (Supplementary Figure S4C) or *GADD45A* (Supplementary Figure S4D) intron fragments. These results confirm that ZBRK1, KAP-1 and LCoR are capable of reporter gene repression through a region containing the ZBRK1 recognition sequence. Both LCoR and KAP-1 can repress transcription through associations with HDACs (6,8,13). However, the HDAC inhibitor trichostatin A (Supplementary Figure S4E) did not abrogate repression, consistent with the transcriptional silencing by these regions being HDAC independent.

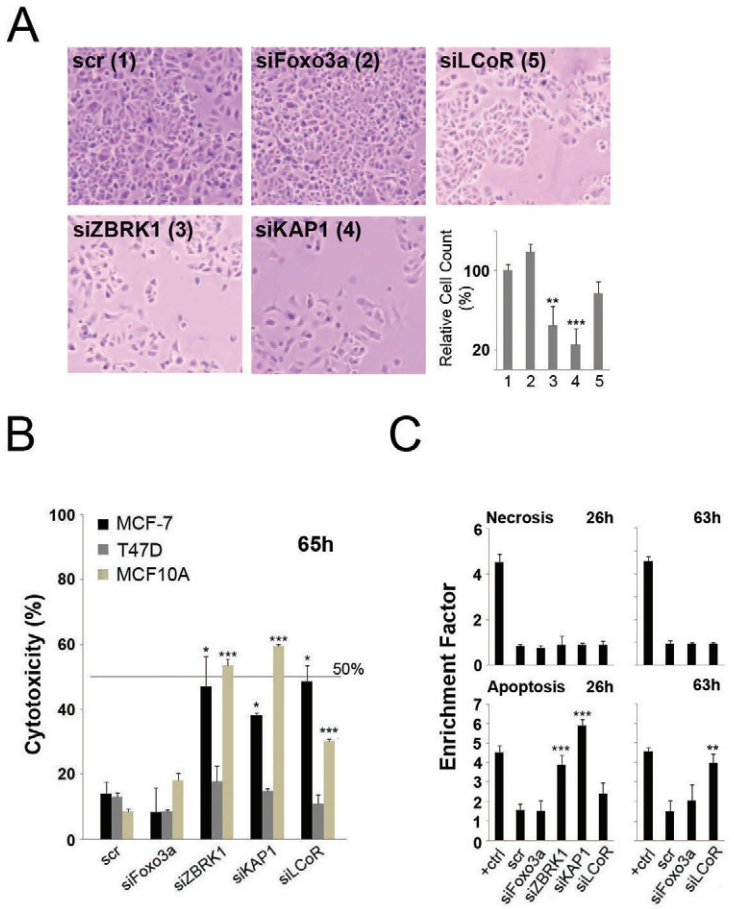

Figure 5. Gene knockdowns increase apoptosis in specific breast cancer cells. (**A**) siRNA-mediated gene knockdowns were stained with trypan blue at 48 h and images were captured by microscopy. Cells were counted and calculated as a percent change from scrambled (scr) control. (**B**) Cytotoxicity of MCF-7, MCF10A and T47D cells was detected with a cytotoxicity detection kit (LDH assay) after siRNA-mediated gene knockdowns. One-way ANOVA followed by the Tukey test for multiple comparisons was performed to determine statistical significance. (**C**) Cell death was characterized using a Cell Death ELISA kit (Roche) after 26 and 65-h gene knockdowns. The kit was supplied with a positive control and the result was included in the figure. One-way ANOVA followed by the Tukey test for multiple comparisons was performed to determine statistical significance.

Ablation of ZBRK1, KAP-1 and LCoR increases apoptosis in specific breast cancer cells

SiRNA-mediated knockdowns of ZBRK1 or KAP-1 consistently reduced the number of adherent MCF-7 or MCF10A cells after 48 h (Figure 5A; data not shown). While not statistically significant at 48 h, the reduction in adherent MCF-7 cells after LCoR ablation was visible 72 h after knockdown (Figure 5A and Supplementary Figure S5A). Note that during knockdowns, loss of ZBRK1 or KAP-1 is observed as early as 24 h after siRNA transfection (Supplementary Figure S5B), whereas depletion of LCoR does not appear before 48–72 h (Figure 2A; data not shown) possibly explaining the delay in response. FoxO3A expression was also ablated as a control for potential transfection reagent cytotoxicity, and had no significant effect on adherent cell numbers at either time point (Figure 5A and Supplementary Figure S5A).

To determine whether ZBRK1, KAP-1 or LCoR ablation was causing cell death, we measured release of LDH into the media, which occurs due to loss of membrane integrity. Disruption of membrane integrity of mock transfected cells (transfection reagent without siRNA) with 1% Triton X-100 was used as a control for maximal LDH release. These experiments revealed that the cytotoxicity caused by loss of ZBRK1, KAP-1 or LCoR expression in MCF-7 and MCF10A cells reached around 50% of the positive control, whereas ablation of FoxO3A expression had no effect on LDH release (Figure 5B). In contrast, similar knockdowns in T47D cells (Supplementary Figure S2A) did not change either cell numbers (data not shown) or cell viability (Figure 5B). To better characterize the mechanism causing cell death, we used a Cell Death ELISA kit, which measures apoptosis and necrosis. Results from these experiments show that 26 h after ZBRK1 or KAP-1 knockdown there was an increase in apoptosis in MCF-7 cells, and 63 h after knockdown, LCoR caused an increase in apoptosis as well, whereas ablation of FoxO3A had no effect (Figure 5C).

Regulation of *FGF2* expression by ZBRK1, KAP-1 and LCoR controls MCF-7 cell viability

Previous studies revealed that increased levels of the secreted form of FGF2 reduce MCF-7 cell viability (21–23). As presented above, ablation of LCoR, KAP-1 or ZBRK1 did not lead to an apoptotic response in T47D cells, which do not express *FGF2*. To determine if increased FGF2 secretion resulted from ablation of ZBRK1, KAP-1 or LCoR in MCF-7 cells, we performed an ELISA for FGF2 in media supernatants. FGF2 secretion was enhanced about 4-fold 48 h after ablation of ZBRK1 or KAP-1, whereas another 24 h were necessary to further elevate (3-fold) FGF2 secretion after LCoR ablation (Figure 6A), consistent with delayed loss of LCoR expression (Supplementary Figure S5B).

Elevated expression of FGF2 in MCF-7 cells has also been associated with reduced Bcl-2 activity and increased apoptosis (23). Reduced Bcl-2 can enhance effector caspase activity and cause cell death (34). MCF-7 cells do not express the effector caspase-3 (35), although apoptosis can occur through effector caspase-7 (36,37). Using the Caspase-Glo 3/7 assay, we observed an increase in caspase activity 24 h after ZBRK1 or KAP-1 ablation, whereas a 2-fold increase in caspase activity was detected 65 h after LCoR depletion (Figure 6B), further confirming apoptosis in MCF-7 cells after gene knockdowns. Ablation of FoxO3A was used as a control for an NS increase in caspase activity, and revealed no change at either time point (Figure 6B). Thus, the apoptosis observed after gene knockdowns correlates with an increase in caspase activity.

To determine if loss of cell viability could be reversed by blocking the enhanced *FGF2* expression resulting from knockdowns, we cotransfected siRNA targeting *FGF2*. The *FGF2* siRNA effectively inhibited the increase in *FGF2* mRNA observed after gene knockdowns and did not interfere with the reduction of transcripts encoding ZBRK1, KAP-1 or LCoR (Figure 6C). Concurrent knockdown of FGF2 significantly reduced the cytotoxic effect of ZBRK1, KAP-1 or LCoR ablation, but had no effect on cell viability in FoxO3A-deficient cells (Figure 6D). To further investigate whether enhanced secretion of FGF2 decreases MCF-7 cell viability, we treated cells transfected with siRNAs targeting *ZBRK1*, *KAP1* or *LCOR* with suramin sodium, which inhibits cell surface binding of FGF2 with its receptor. The inhibitor significantly reduced the cytotoxic effects of ZBRK1, KAP-1 or LCoR ablation (Figure 6E), providing further evidence that enhanced FGF2 expression and secretion contributes to the cell death observed after ablation of ZBRK1, KAP-1 or LCoR.

As mentioned above, knockdowns of *ZBRK1* and *KAP1* in MCF-7 or MCF10A cells led to increased *MMP9* expression (Figure 2B and C), although depletion of LCoR had a non-significant effect in MCF-7 cells. Overexpression of *MMP9* in cervical cancer has been shown to enhance tumor growth and progression (19), raising the possibility that its elevated expression in knockdown experiments may partially counteract the effects of FGF2 overexpression caused by *ZBRK1*, *KAP1* or *LCOR* ablation in breast cell lines. Concurrent knockdown of *MMP9* with *ZBRK1*, *KAP1* or *LCOR* in MCF-7 cells (Supplementary Figure S6A) led to modest but significant increases in cytotoxicity as measured with an LDH assay (Supplementary Figure S6B). This suggests that enhanced expression of MMP9 occurring upon ZBRK1, KAP-1 or LCoR ablation attenuates the effect of elevated FGF2 expression.

FGF2 is not coexpressed with ZBRK1, KAP-1 or LCoR in malignant breast tissue

In order to compare the expression patterns of ZBRK1, KAP-1, LCoR and FGF2 in breast cancer tissue, we analyzed tissue microarrays containing a variety of breast tissues, normal and malignant, for expression of all four proteins. Tissue samples were scored as previously described (30), where the score is determined as staining intensity x PP (percentage of positive cells); staining intensity of 0 is negative; 1, weak; 2, moderate; and 3, strong. PP was defined as 0 if negative; 1, 10% positive cells; 2, 11–50% positive cells; 3, 51–80% positive cells; and 4, more than 80% positive cells (score limits 1: minimum; 12: maximum). Although FGF2 was readily detected in melanoma (Supplementary Figure S7A), which served as a positive control, we failed to detect its expression in nearly all malignant breast tissues. Expression of modest levels was observed in within fibroadenoma samples but was confined to normal ductal epithelia (Figure 7A and Supplementary Figure S7B), consistent with previous observations (27). These cells, which are in close proximity to luminal structures, may be undergoing apoptosis (38). Normal ductal epithelial cells did express appreciable levels of KAP-1, ZBRK1 and LCoR, although LCoR expression was variable and mostly cytoplasmic (Figure 7A). Expression of ZBRK1, KAP-1 or LCoR was detected in a majority of malignancies probed (Supplementary Figure S7B). For example, breast medullary carcinoma, a type of invasive ductal carcinoma that accounts for 5% of all breast cancers (39), widely expressed KAP-1, whereas no FGF2 was detected (Figure 7B). Although individual carcinoma cells did not appear to express higher levels of the protein than normal cells, LCoR expression was more widely distributed and nuclear in medullary carcinoma than in normal ductal epithelial cells (Figure 7A and B). Out of 100 tissue samples probed (50 cases each in duplicate: eight invasive ductal carcinoma, eight mucinous carcinoma, six medullary carcinoma, four malignant Paget's disease, two carcinosarcoma, eight cystosarcoma phyllodes, eight fibroadenoma and six cancer adjacent normal breast tissue) with each antibody, we found no example of coexpression in malignant tissue of FGF2 with any of the transcriptional regulators studied here (Supplementary Figure S7B).

Analysis of normal versus cancer tissue did not provide evidence for overexpression of any of the coregulators in malignant tissue, whereas a significant reduction in expression of FGF2 was detected (Supplementary Figure S7C; compare Figure 7A to Supplementary Figure S7A), consistent with previous reports (25–28,40). In order to further explore the relationships between expression of FGF2 and ZBRK1 (ZNF350) and KAP-1 (TRIM28) and LCoR, we expanded our analysis to the larger data set of the cancer genome atlas (TCGA) (https://tcga-data.nci.nih.gov/). Using the TCGA IlluminaHiSeq breast invasive carcinoma

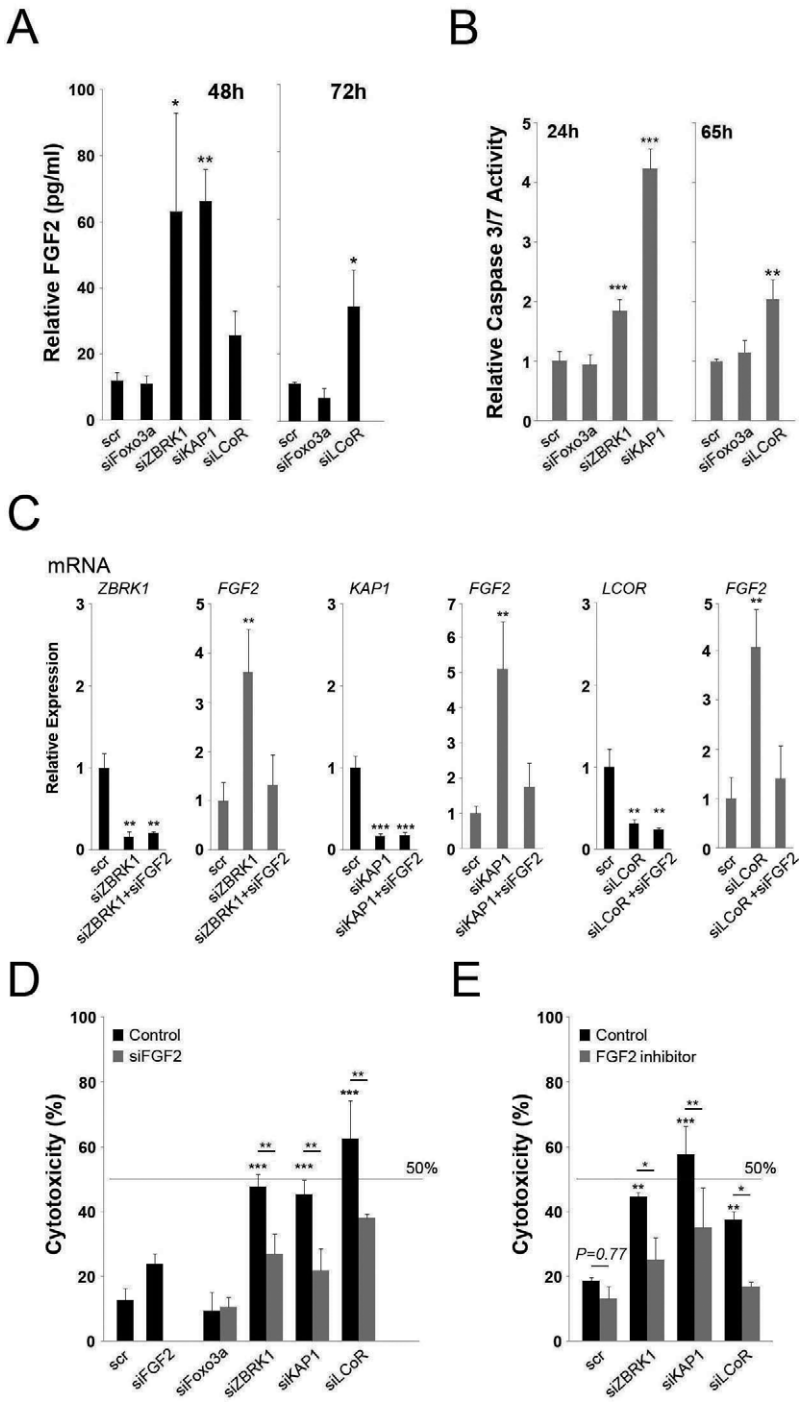

Figure 6. Gene knockdowns increase FGF2 secretion and alter MCF-7 cell viability. (**A**) FGF2 secretion was measured by ELISA after 48-h or 72-h siRNA-mediated gene knockdowns and normalized to cell counts at each time point. (**B**) Caspase 3/7 activity was measured with a caspase 3/7 activity detection kit after 24 or 65-h siRNA-mediated gene knockdowns. (**C**) Confirmation of abrogation of *FGF2* mRNA increase after gene knockdowns. RT-qPCR of joint (regulator+FGF2) siRNA-mediated knockdowns in MCF-7 cells. (**D**) Cytotoxicity of cells as measured by the LDH assay (Roche) 65 h after gene knockdowns. (**E**) Cytotoxicity of cells as measured by the LDH assay (Roche) 65 h after gene knockdowns and incubation with water (control) or 100-μM suramin sodium (FGF2 inhibitor). One-way ANOVA followed by the Tukey test for multiple comparisons was performed to determine statistical significance in all cases.

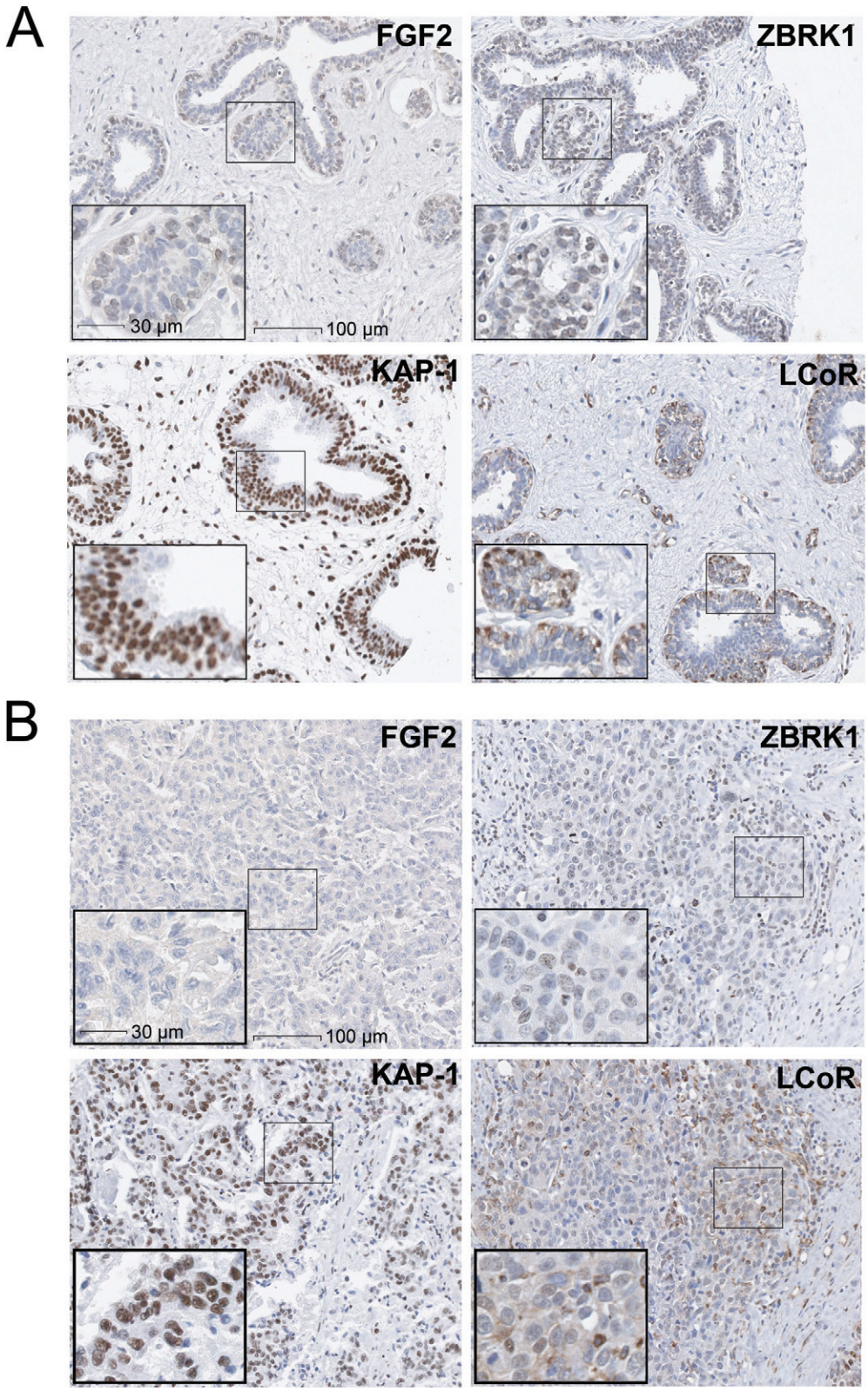

Figure 7. Absence of coexpression of FGF2 and transcriptional regulators in malignant breast tissue microarray. Digital brightfield images of antibody staining of (**A**) fibroadenoma or (**B**) medullary carcinoma samples captured with NanoZoomer® 2.0-HT scanner. Images are at a magnification of ×40 while insets are at ×63.

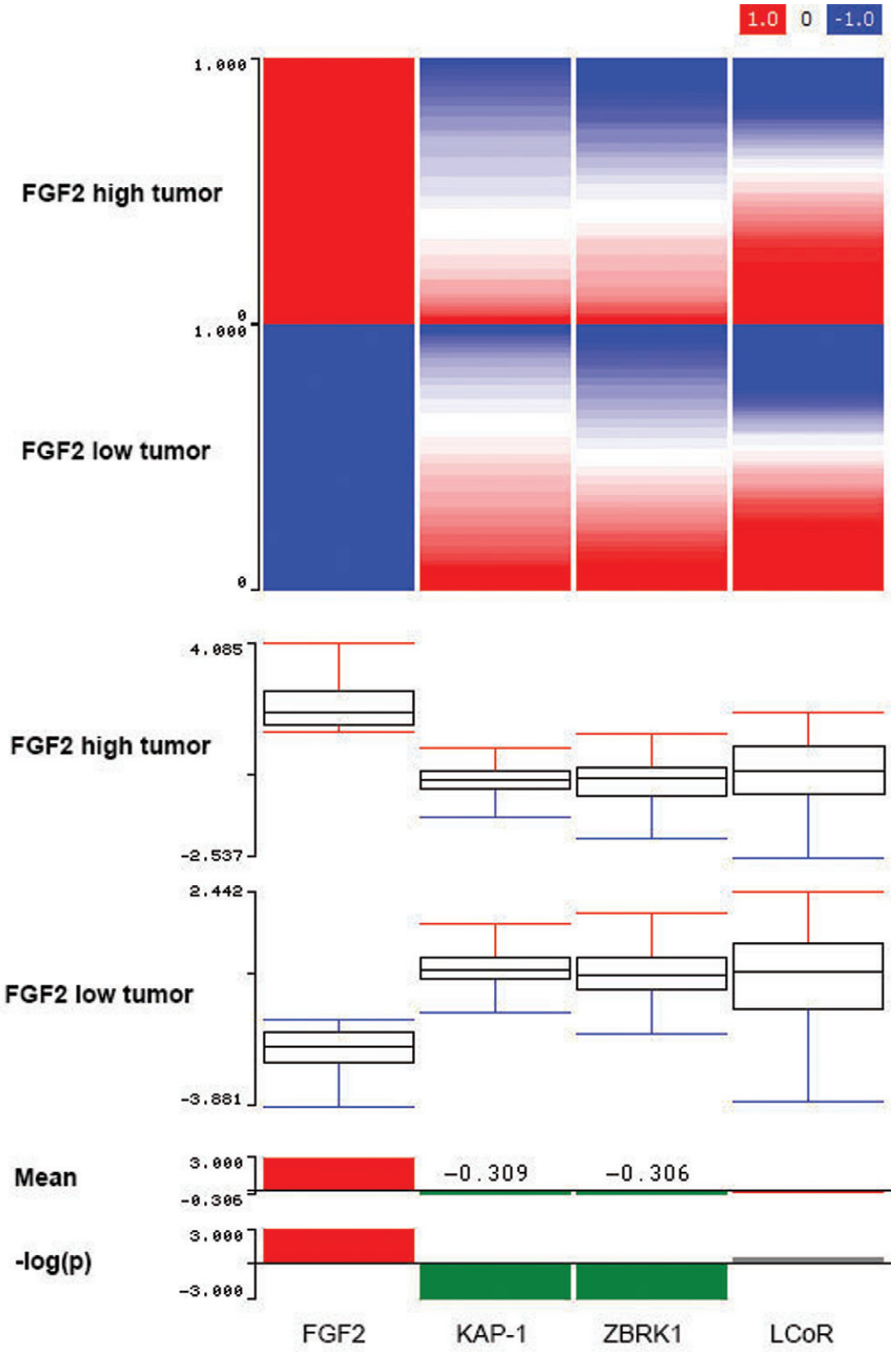

Figure 8. FGF2 expression is inversely correlated with KAP-1 and ZBRK1 expression in the TGCA data set of breast invasive carcinoma. (Top) Gene expression in breast invasive carcinoma was normalized to normal control tissue, and samples were gated for high and low expressions of FGF2, where red indicates upregulation and blue indicates downregulation. (Middle) Box-plot of this analysis of these samples demonstrates that the mean expression for KAP-1 and ZBRK1 relative to control tissue was inversely correlated with the expression of FGF2 in both sample populations. (Bottom) In samples that expressed high FGF2, the mean expression of KAP-1 and ZBRK1 was negative (values indicated on bar graph) relative to control tissue and statistically significant at $P = 0.001$ as determined by student's *t*-test.

RNAseq database ($N = 1106$) and separating tumors based on high or low *FGF2* expression, statistically significant inverse relationships were observed between the expression of *ZBRK1* or *KAP1* and *FGF2* mRNAs (Figure 8). Collectively, the above data suggest that the expression of the coregulators and FGF2 is mutually exclusive in malignant breast tissue and that an inverse relationship exists between the expression of *ZBRK1* and *KAP1* mRNA and that of *FGF2* in breast invasive carcinoma.

DISCUSSION

We have identified a novel and direct association of the corepressor LCoR with the coregulator KAP-1 in a C-terminal region of LCoR that is distinct from the domains recognized by CtBPs and HDACs. These findings link LCoR function to regulation of transcription by C_2H_2 zinc-finger proteins. The C_2H_2 zinc-finger-containing gene family is one of the largest families in metazoan genomes (41), and over half of the zinc-finger genes in the human genome also contain an N-terminal KRAB domain (42). KAP-1 binds directly through its RBCC domain to several KRAB-containing C_2H_2 zinc-finger TFs (13), and ChIPseq studies revealed numerous KAP-1 recruitment sites in the human genome (9). KAP-1 is also widely expressed during embryonic development and in the adult, and its disruption in mice is embryonic lethal (13,43). Similarly, LCoR is expressed as early as the 2-cell stage of embryonic development (5), suggesting a potential early link of LCoR function to coregulation of transcription by C_2H_2 zinc-finger proteins during development. Using ZBRK1 as a model C_2H_2 zinc-finger protein, we confirmed coassociation of LCoR, KAP-1 and ZBRK1 by ChIP and reChIP assays at a previously characterized intronic motif in the *GADD45A* gene and at a novel almost identical motif in the *FGF2* gene. We also detected the binding of the histone methyltransferase SETDB1 and enrichment of the repressive mark H3K9Me3 associated with KAP-1 function (12,13) at both ZBRK1 motifs under conditions where ZBRK1, KAP-1 and LCoR repressed gene transcription. The association of the novel *FGF2* motif with SETDB1 and H3K9 methylation was supported by ENCODE ChIPseq data, which revealed elevated H3K9Me3 levels in a region encompassing the motif. Ablation of ZBRK1, KAP-1 or LCoR expression led to enhanced *GADD45A* and *FGF2* expression in MCF10A and MCF-7 cells. ENCODE data confirmed our results with *FGF2*.

Little is known about transcriptional silencing of the *FGF2* gene (44) or the exact cause of reduced FGF2 expression in breast malignancies. Its silencing is of significance, however, because elevated or forced expression of FGF2 in breast cells stunts growth or induces apoptosis (21–24,45). Significantly, we found that *FGF2* repression by ZBRK1, KAP-1 or LCoR contributed to both tumorigenic (MCF-7) and non-tumorigenic (MCF10A) cell survival, indicating that these transcriptional regulators can silence *FGF2* in malignant and non-malignant cells. As the region in which FGF2 expression was detected in breast tissue microarrays (normal ductal epithelial cells) may be undergoing apoptosis which would maintain luminal space (38), it suggests that apoptosis caused by active regulation of the *FGF2* gene might contribute to shape these structures. Moreover, although gene knockdowns of the transcriptional regulators revealed an increase in *MMP9* that promotes cell growth (19), the increase was insufficient to prevent cell death and was only slightly protective, indicating a predominant effect of induced FGF2 expression in these cells. While *FGF2* was detected in MCF-7 and MCF10A cells, its expression was undetectable in T47D cells under any conditions tested and its profound silencing appeared to be independent of function of the ZBRK1/KAP-1/LCoR complex, suggesting that *FGF2* gene expression can be inhibited by multiple mechanisms in breast cancer. Notably, in this regard, one report found an *FGF2* gene deletion in a breast tumor sample (46).

Probing breast cancer tissue microarrays did not reveal any evidence for overexpression of any of the complex components in the breast cancer samples analyzed. Importantly, however, the microarrays did not reveal any evidence for coexpression of ZBRK1, KAP-1 or LCoR and FGF2. We also analyzed the much larger TCGA breast invasive carcinoma RNAseq database ($N = 1106$), which revealed a significant inverse relationship between *ZBRK1* or *KAP1* and *FGF2* transcripts. No inverse relationship was found between *FGF2* and *LCOR* mRNAs, although it is important to note that LCoR function may be controlled largely at the protein level. While the analysis of the TCGA data suggests that elevated expression of *ZBRK1* and *KAP1* transcripts contributes to silencing of *FGF2* expression, other mechanisms may lead to increased repressor activity of the complex. For example, function of the ZBRK1/KAP-1/LCoR may be controlled by upstream signal transduction pathways acting through complex subunits in addition to effects of altered expression levels of the components. Notably in this regard, association of KAP-1 with cofactors can be regulated by phosphorylation/dephosphorylation and sumoylation, affecting its function (47–50). On the other hand, nothing is known about potential post-translational mechanisms controlling LCoR or ZBRK1 function, although there is evidence that sumoylation status can alter C_2H_2 zinc-finger protein associations with coregulators (51). FGF2 has also been shown to induce apoptosis in the early primary culture of rat cortical neurons (52), and a hippocampal cell line and primary cell cultures derived from the hippocampus (53), raising the possibility that FGF2-mediated apoptosis regulated by this transcriptional complex may not be limited to breast tissue, as both KAP-1 and LCoR are highly expressed in neuronal tissues (5,9).

Many examples exist in the literature of other types of cells in which an association between LCoR and KAP-1 might be relevant in terms of regulation of C_2H_2 zinc-finger protein-mediated transcription. The most obvious candidates would be cells in which an interaction between ZBRK1 and KAP-1 has already been established such as hybrid Burkitt lymphoblastoid cells (14) or human embryonic kidney cells (16). However, if the LCoR–KAP-1 complex was recruited to additional C_2H_2 zinc-finger proteins, it may regulate numerous other genes under a wide variety of conditions. Notably, KAP-1 interacts with zinc-finger protein 274 in human chronic myelogenous leukemia cells (54), zinc-finger protein 57 in mouse embryonic stem cells (55) and zinc-finger protein 809 in mouse embryonic car-

cinoma cells (56), to name just a few. The complex would then function to regulate processes that would range from embryogenesis to retroviral silencing (55,56), which is entirely plausible given the early and widespread expression of both LCoR and KAP-1 (5,13).

In conclusion, we have identified a novel interaction between the corepressors of transcription LCoR and KAP-1, which are recruited to ZBRK1 binding sites to silence gene expression and promote breast cell survival. Given the broad expression of LCoR and KAP-1, it is possible that a complex containing LCoR and KAP-1 might have functions that extend beyond cell survival, which would be mediated by interactions with different C_2H_2 zinc-finger proteins expressed in a variety of tissues.

SUPPLEMENTARY DATA

Supplementary Data are available at NAR Online.

ACKNOWLEDGMENTS

We would like to thank Ms Yolande Bastien for advice on GST pulldowns and Ms Julie Hisinger (Université de Montréal) for preliminary work on tissue microarrays.

FUNDING

This study was funded by a grant from the Canadian Institute of Health Research (CIHR) [Grant number MT-11704] and a grant from the Natural Sciences and Engineering Research Council (NSERC) [Grant number RGPGP-2014-00084] to J.H.W.; M.V and M.B were supported by doctoral and postdoctoral fellowships, respectively, from the Fonds de Recherche du Québec-Santé [FRSQ]. Funding for open access charge: Canadian Institutes of Health Research.
Conflict of interest statement. None declared.

REFERENCES

1. Kouzarides,T. (2007) Chromatin modifications and their function. *Cell*, **128**, 693–705.
2. Smith,E. and Shilatifard,A. (2010) The chromatin signaling pathway: diverse mechanisms of recruitment of histone-modifying enzymes and varied biological outcomes. *Mol. Cell*, **40**, 689–701.
3. Latchman,D.S. (1997) Transcription factors: an overview. *Int. J. Biochem. Cell Biol.*, **29**, 1305–1312.
4. Shi,Y., Sawada,J., Sui,G., Affar el,B., Whetstine,J.R., Lan,F., Ogawa,H., Luke,M.P. and Nakatani,Y. (2003) Coordinated histone modifications mediated by a CtBP co-repressor complex. *Nature*, **422**, 735–738.
5. Fernandes,I., Bastien,Y., Wai,T., Nygard,K., Lin,R., Cormier,O., Lee,H.S., Eng,F., Bertos,N.R., Pelletier,N. *et al.* (2003) Ligand-dependent nuclear receptor corepressor LCoR functions by histone deacetylase-dependent and -independent mechanisms. *Mol. Cell*, **11**, 139–150.
6. Palijan,A., Fernandes,I., Bastien,Y., Tang,L., Verway,M., Kourelis,M., Tavera-Mendoza,L.E., Li,Z., Bourdeau,V., Mader,S. *et al.* (2009) Function of histone deacetylase 6 as a cofactor of nuclear receptor coregulator LCoR. *J. Biol. Chem.*, **284**, 30264–30274.
7. Palijan,A., Fernandes,I., Verway,M., Kourelis,M., Bastien,Y., Tavera-Mendoza,L.E., Sacheli,A., Bourdeau,V., Mader,S. and White,J.H. (2009) Ligand-dependent corepressor LCoR is an attenuator of progesterone-regulated gene expression. *J. Biol. Chem.*, **284**, 30275–30287.
8. Calderon,M.R., Verway,M., An,B.S., DiFeo,A., Bismar,T.A., Ann,D.K., Martignetti,J.A., Shalom-Barak,T. and White,J.H. (2012) Ligand-dependent corepressor (LCoR) recruitment by Kruppel-like factor 6 (KLF6) regulates expression of the cyclin-dependent kinase inhibitor CDKN1A gene. *J. Biol. Chem.*, **287**, 8662–8674.
9. Iyengar,S., Ivanov,A.V., Jin,V.X., Rauscher,F.J. III and Farnham,P.J. (2011) Functional analysis of KAP1 genomic recruitment. *Mol. Cell. Biol.*, **31**, 1833–1847.
10. Groner,A.C., Meylan,S., Ciuffi,A., Zangger,N., Ambrosini,G., Denervaud,N., Bucher,P. and Trono,D. (2010) KRAB-zinc finger proteins and KAP1 can mediate long-range transcriptional repression through heterochromatin spreading. *PLoS Genet.*, **6**, e1000869.
11. O'Geen,H., Squazzo,S.L., Iyengar,S., Blahnik,K., Rinn,J.L., Chang,H.Y., Green,R. and Farnham,P.J. (2007) Genome-wide analysis of KAP1 binding suggests autoregulation of KRAB-ZNFs. *PLoS Genet.*, **3**, e89.
12. Schultz,D.C., Ayyanathan,K., Negorev,D., Maul,G.G. and Rauscher,F.J. III (2002) SETDB1: a novel KAP-1-associated histone H3, lysine 9-specific methyltransferase that contributes to HP1-mediated silencing of euchromatic genes by KRAB zinc-finger proteins. *Genes Dev.*, **16**, 919–932.
13. Iyengar,S. and Farnham,P.J. (2011) KAP1 protein: an enigmatic master regulator of the genome. *J. Biol. Chem.*, **286**, 26267–26276.
14. Liao,G., Huang,J., Fixman,E.D. and Hayward,S.D. (2005) The Epstein-Barr virus replication protein BBLF2/3 provides an origin-tethering function through interaction with the zinc finger DNA binding protein ZBRK1 and the KAP-1 corepressor. *J. Virol.*, **79**, 245–256.
15. Lee,Y.K., Thomas,S.N., Yang,A.J. and Ann,D.K. (2007) Doxorubicin down-regulates Kruppel-associated box domain-associated protein 1 sumoylation that relieves its transcription repression on p21WAF1/CIP1 in breast cancer MCF-7 cells. *J. Biol. Chem.*, **282**, 1595–1606.
16. Nishitsuji,H., Abe,M., Sawada,R. and Takaku,H. (2012) ZBRK1 represses HIV-1 LTR-mediated transcription. *FEBS Lett.*, **586**, 3562–3568.
17. Zheng,L., Pan,H., Li,S., Flesken-Nikitin,A., Chen,P.L., Boyer,T.G. and Lee,W.H. (2000) Sequence-specific transcriptional corepressor function for BRCA1 through a novel zinc finger protein, ZBRK1. *Mol. Cell*, **6**, 757–768.
18. Ahmed,K.M., Tsai,C.Y. and Lee,W.H. (2010) Derepression of HMGA2 via removal of ZBRK1/BRCA1/CtIP complex enhances mammary tumorigenesis. *J Biol Chem*, **285**, 4464–4471.
19. Lin,L.F., Chuang,C.H., Li,C.F., Liao,C.C., Cheng,C.P., Cheng,T.L., Shen,M.R., Tseng,J.T., Chang,W.C., Lee,W.H. *et al.* (2010) ZBRK1 acts as a metastatic suppressor by directly regulating MMP9 in cervical cancer. *Cancer Res.*, **70**, 192–201.
20. Furuta,S., Wang,J.M., Wei,S., Jeng,Y.M., Jiang,X., Gu,B., Chen,P.L., Lee,E.Y. and Lee,W.H. (2006) Removal of BRCA1/CtIP/ZBRK1 repressor complex on ANG1 promoter leads to accelerated mammary tumor growth contributed by prominent vasculature. *Cancer Cell*, **10**, 13–24.
21. Fenig,E., Szyper-Kravitz,M., Yerushalmi,R., Lahav,M., Beery,E., Wasserman,L., Gutman,H. and Nordenberg,J. (2002) Basic fibroblast growth factor mediated growth inhibition in breast cancer cells is independent of ras signaling pathway. *Oncol. Rep.*, **9**, 875–877.
22. Liu,D., Buluwela,L., Ali,S., Thomson,S., Gomm,J.J. and Coombes,R.C. (2001) Retroviral infection of the FGF2 gene into MCF-7 cells induces branching morphogenesis, retards cell growth and suppresses tumorigenicity in nude mice. *Eur. J. Cancer*, **37**, 268–280.
23. Maloof,P., Wang,Q., Wang,H., Stein,D., Denny,T.N., Yahalom,J., Fenig,E. and Wieder,R. (1999) Overexpression of basic fibroblast growth factor (FGF-2) downregulates Bcl-2 and promotes apoptosis in MCF-7 human breast cancer cells. *Breast Cancer Res. Treat.*, **56**, 153–167.
24. Korah,R.M., Sysounthone,V., Scheff,E. and Wieder,R. (2000) Intracellular FGF-2 promotes differentiation in T-47D breast cancer cells. *Biochem. Biophys. Res. Commun.*, **277**, 255–260.
25. Luqmani,Y.A., Graham,M. and Coombes,R.C. (1992) Expression of basic fibroblast growth factor, FGFR1 and FGFR2 in normal and malignant human breast, and comparison with other normal tissues. *Br. J. Cancer*, **66**, 273–280.
26. Smith,J., Yelland,A., Baillie,R. and Coombes,R.C. (1994) Acidic and basic fibroblast growth factors in human breast tissue. *Eur. J. Cancer*, **30A**, 496–503.

27. Yiangou,C., Gomm,J.J., Coope,R.C., Law,M., Luqmani,Y.A., Shousha,S., Coombes,R.C. and Johnston,C.L. (1997) Fibroblast growth factor 2 in breast cancer: occurrence and prognostic significance. *Br. J. Cancer*, **75**, 28–33.
28. Soufla,G., Porichis,F., Sourvinos,G., Vassilaros,S. and Spandidos,D.A. (2006) Transcriptional deregulation of VEGF, FGF2, TGF-beta1, 2, 3 and cognate receptors in breast tumorigenesis. *Cancer Lett.*, **235**, 100–113.
29. Germain-Desprez,D., Bazinet,M., Bouvier,M. and Aubry,M. (2003) Oligomerization of transcriptional intermediary factor 1 regulators and interaction with ZNF74 nuclear matrix protein revealed by bioluminescence resonance energy transfer in living cells. *J. Biol. Chem.*, **278**, 22367–22373.
30. Friedrichs,K., Gluba,S., Eidtmann,H. and Jonat,W. (1993) Overexpression of p53 and prognosis in breast cancer. *Cancer*, **72**, 3641–3647.
31. Wang,J., Scully,K., Zhu,X., Cai,L., Zhang,J., Prefontaine,G.G., Krones,A., Ohgi,K.A., Zhu,P., Garcia-Bassets,I. *et al.* (2007) Opposing LSD1 complexes function in developmental gene activation and repression programmes. *Nature*, **446**, 882–887.
32. Tran,H., Brunet,A., Grenier,J.M., Datta,S.R., Fornace,A.J. Jr, DiStefano,P.S., Chiang,L.W. and Greenberg,M.E. (2002) DNA repair pathway stimulated by the forkhead transcription factor FOXO3a through the Gadd45 protein. *Science*, **296**, 530–534.
33. Bernstein,B.E., Birney,E., Dunham,I., Green,E.D., Gunter,C. and Snyder,M. (2012) An integrated encyclopedia of DNA elements in the human genome. *Nature*, **489**, 57–74.
34. Marsden,V.S., O'Connor,L., O'Reilly,L.A., Silke,J., Metcalf,D., Ekert,P.G., Huang,D.C., Cecconi,F., Kuida,K., Tomaselli,K.J. *et al.* (2002) Apoptosis initiated by Bcl-2-regulated caspase activation independently of the cytochrome c/Apaf-1/caspase-9 apoptosome. *Nature*, **419**, 634–637.
35. Mooney,L.M., Al-Sakkaf,K.A., Brown,B.L. and Dobson,P.R. (2002) Apoptotic mechanisms in T47D and MCF-7 human breast cancer cells. *Br. J. Cancer*, **87**, 909–917.
36. Semenov,D.V., Aronov,P.A., Kuligina,E.V., Potapenko,M.O. and Richter,V.A. (2004) Oligonucleosome DNA fragmentation of caspase 3 deficient MCF-7 cells in palmitate-induced apoptosis. *Nucleosides Nucleotides Nucleic Acids*, **23**, 831–836.
37. Cuvillier,O., Nava,V.E., Murthy,S.K., Edsall,L.C., Levade,T., Milstien,S. and Spiegel,S. (2001) Sphingosine generation, cytochrome c release, and activation of caspase-7 in doxorubicin-induced apoptosis of MCF7 breast adenocarcinoma cells. *Cell Death Differ.*, **8**, 162–171.
38. Debnath,J., Mills,K.R., Collins,N.L., Reginato,M.J., Muthuswamy,S.K. and Brugge,J.S. (2002) The role of apoptosis in creating and maintaining luminal space within normal and oncogene-expressing mammary acini. *Cell*, **111**, 29–40.
39. Linda,A., Zuiani,C., Girometti,R., Londero,V., Machin,P., Brondani,G. and Bazzocchi,M. (2010) Unusual malignant tumors of the breast: MRI features and pathologic correlation. *Eur. J. Radiol.*, **75**, 178–184.
40. Colomer,R., Aparicio,J., Montero,S., Guzman,C., Larrodera,L. and Cortes-Funes,H. (1997) Low levels of basic fibroblast growth factor (bFGF) are associated with a poor prognosis in human breast carcinoma. *Br. J. Cancer*, **76**, 1215–1220.
41. Seetharam,A. and Stuart,G.W. (2013) A study on the distribution of 37 well conserved families of C2H2 zinc finger genes in eukaryotes. *BMC Genomics*, **14**, 420.
42. Birtle,Z. and Ponting,C.P. (2006) Meisetz and the birth of the KRAB motif. *Bioinformatics*, **22**, 2841–2845.
43. Cammas,F., Mark,M., Dolle,P., Dierich,A., Chambon,P. and Losson,R. (2000) Mice lacking the transcriptional corepressor TIF1beta are defective in early postimplantation development. *Development*, **127**, 2955–2963.
44. Basilico,C. and Moscatelli,D. (1992) The FGF family of growth factors and oncogenes. *Adv. Cancer Res.*, **59**, 115–165.
45. Korah,R.M., Sysounthone,V., Golowa,Y. and Wieder,R. (2000) Basic fibroblast growth factor confers a less malignant phenotype in MDA-MB-231 human breast cancer cells. *Cancer Res.*, **60**, 733–740.
46. Schmitt,J.F., Susil,B.J. and Hearn,M.T. (1996) Aberrant FGF-2, FGF-3, FGF-4 and C-erb-B2 gene copy number in human ovarian, breast and endometrial tumours. *Growth Factors*, **13**, 19–35.
47. Chang,C.W., Chou,H.Y., Lin,Y.S., Huang,K.H., Chang,C.J., Hsu,T.C. and Lee,S.C. (2008) Phosphorylation at Ser473 regulates heterochromatin protein 1 binding and corepressor function of TIF1beta/KAP1. *BMC Mol. Biol.*, **9**, 61.
48. Ziv,Y., Bielopolski,D., Galanty,Y., Lukas,C., Taya,Y., Schultz,D.C., Lukas,J., Bekker-Jensen,S., Bartek,J. and Shiloh,Y. (2006) Chromatin relaxation in response to DNA double-strand breaks is modulated by a novel ATM- and KAP-1 dependent pathway. *Nat. Cell Biol.*, **8**, 870–876.
49. White,D.E., Negorev,D., Peng,H., Ivanov,A.V., Maul,G.G. and Rauscher,F.J. III (2006) KAP1, a novel substrate for PIKK family members, colocalizes with numerous damage response factors at DNA lesions. *Cancer Res.*, **66**, 11594–11599.
50. Goodarzi,A.A., Kurka,T. and Jeggo,P.A. (2011) KAP-1 phosphorylation regulates CHD3 nucleosome remodeling during the DNA double-strand break response. *Nat. Struct. Mol. Biol.*, **18**, 831–839.
51. Oishi,Y., Manabe,I., Tobe,K., Ohsugi,M., Kubota,T., Fujiu,K., Maemura,K., Kubota,N., Kadowaki,T. and Nagai,R. (2008) SUMOylation of Kruppel-like transcription factor 5 acts as a molecular switch in transcriptional programs of lipid metabolism involving PPAR-delta. *Nat. Med.*, **14**, 656–666.
52. Yagami,T., Takase,K., Yamamoto,Y., Ueda,K., Takasu,N., Okamura,N., Sakaeda,T. and Fujimoto,M. (2010) Fibroblast growth factor 2 induces apoptosis in the early primary culture of rat cortical neurons. *Exp. Cell Res.*, **316**, 2278–2290.
53. Eves,E.M., Skoczylas,C., Yoshida,K., Alnemri,E.S. and Rosner,M.R. (2001) FGF induces a switch in death receptor pathways in neuronal cells. *J. Neurosci.*, **21**, 4996–5006.
54. Frietze,S., O'Geen,H., Blahnik,K.R., Jin,V.X. and Farnham,P.J. (2010) ZNF274 recruits the histone methyltransferase SETDB1 to the 3′ ends of ZNF genes. *PLoS ONE*, **5**, e15082.
55. Quenneville,S., Verde,G., Corsinotti,A., Kapopoulou,A., Jakobsson,J., Offner,S., Baglivo,I., Pedone,P.V., Grimaldi,G., Riccio,A. *et al.* (2011) In embryonic stem cells, ZFP57/KAP1 recognize a methylated hexanucleotide to affect chromatin and DNA methylation of imprinting control regions. *Mol. Cell*, **44**, 361–372.
56. Wolf,D. and Goff,S.P. (2009) Embryonic stem cells use ZFP809 to silence retroviral DNAs. *Nature*, **458**, 1201–1204.